

# Cost-Effective Single Step Cofiring Process for Manufacturing Solid Oxide Fuel Cells Using HSC™ Anode

**Kyung Joong Yoon**

Department of Manufacturing Engineering,  
Boston University,  
15 Saint Mary's Street,  
Brookline, MA 02446

**Guosheng Ye**

BTU International, Inc.,  
23 Esquire Road,  
North Billerica, MA 01862

**Srikanth Gopalan**

**Uday B. Pal**

Department of Manufacturing Engineering,  
Boston University,  
15 Saint Mary's Street,  
Brookline, MA 02446

*The anode-supported planar solid oxide fuel cell (SOFC) was fabricated by a cost-effective single step cofiring process using high shear compaction (HSC)™ anode substrate. The HSC™ process is a novel ceramic tape fabrication technique, which offers advantages in low-cost and high-volume production of the anode substrates over the conventional tape forming processes. The cell was comprised of a porous HSC™ Ni + 8 mol % yttria-stabilized zirconia (YSZ) anode substrate, a porous Ni + YSZ anode barrier layer, a porous and fine-grained Ni + YSZ anode active layer, a dense YSZ electrolyte, a porous and fine-grained Ca-doped LaMnO<sub>3</sub> (LCM) + YSZ composite cathode active layer, and a porous LCM cathode current collector layer. The fabrication process involved wet powder spraying of the anode barrier layer over the HSC™ anode substrate followed by screen-printing of the remaining component layers. The cell was then cofired at 1340 °C for 2 h. The microstructure and the open circuit voltage of the cell confirmed that the cell was crack-free and leak-tight. The cofired cell showed a stable and acceptable electrochemical performance at 800 °C under humidified hydrogen (3–60% H<sub>2</sub>O) as fuel and air as oxidant. The anode active layer with finer and less porous microstructure increased the triple phase boundary length and improved cell performance under conditions that simulated higher fuel utilization. The material system and fabrication process presented in this work offers great advantage in low-cost and high-volume production of SOFCs, and it can be the basis for scale-up and successful commercialization of the SOFC technology. [DOI: 10.1115/1.3177449]*

*Keywords: solid oxide fuel cells (SOFCs), high shear compaction (HSC), wet powder spray (WPS), screen-printing, cofiring, fuel utilization*

## 1 Introduction

SOFCs represent one of the most environmentally clean and versatile means of efficiently converting chemical energy to electrical energy from a wide variety of fuels. At present, one of the major obstacles for the commercialization of SOFC power systems is its high manufacturing cost associated with a complex manufacturing process. The conventional SOFC fabrication techniques involve multiple high-temperature processing steps, which are not amenable to cost-competitive automated manufacturing process. The manufacturing costs of SOFCs can be greatly lowered by employing a single step cofiring technique. To realize the successful single step cofiring of SOFCs, it is critical to lower the sintering temperature of the electrolyte and to minimize the thermal expansion mismatch and sintering shrinkage mismatch between the components. Previously we reported that the anode-supported planar SOFCs were successfully fabricated by the cost-competitive single step cofiring process through the optimization of the materials and process parameters [1–4]. The cells were fabricated by tape casting and lamination of the anode support, screen-printing of the remaining component layers, and cofiring at 1300 °C for 2 h [1–4].

Among the basic SOFC designs, the planar anode-supported SOFCs offer the highest performance [5,6]. In the anode-supported design, anode substrate provides mechanical support, and it is commonly fabricated by a laborious and time consuming process such as tape casting and lamination, which imposes addi-

tional constraints to automation and high-volume production. The HSC™ process is a ceramic tape fabrication technique developed by Ragan Technologies. It is capable of producing tapes of high quality and excellent dimensional tolerance. HSC™ anode tapes have densities and sheet uniformity far beyond other green sheet forming techniques. This process is commonly used in the production of ceramic substrates for electronic applications, and it offers many advantages in SOFC anode manufacturing applications such as low fabrication costs, high production throughput, and good control of shrinkage and thickness [7,8].

The principal objective of the present work was to fabricate anode-supported planar SOFCs by cost-competitive single step cofiring process using the HSC™ anode substrate. The technical challenges and solutions associated with employing the HSC™ anode substrate in single step cofiring process were investigated. The cofired cell was electrochemically tested in the temperature range between 700 °C and 800 °C, and the performance data under the conditions that simulated various fuel utilizations by increasing H<sub>2</sub>O content in the fuel were analyzed.

## 2 Experimental Procedure

**2.1 Cell Fabrication.** Figure 1 shows the schematic of the HSC™ tape formation process. Ceramic powders are mixed in water with the desired amount of binder and dried to form free flowing granules. The powder granules are fed into a hopper in the tape fabrication machine and automatically processed into the forming machine at a metered rate. The forming machine performs several operations such as uniform dispersion, solidification, edge forming, green density and thickness control, and sur-

Manuscript received March 31, 2008; final manuscript received December 12, 2008; published online January 11, 2010. Review conducted by Dr. Masashi Mori.

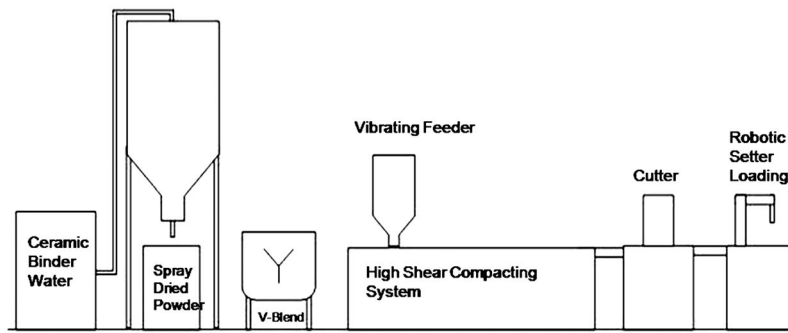


Fig. 1 Schematic of the HSC™ tape formation process

face finish. The tape is completely dry and ready to use as it exits the tape fabrication machine. It feeds directly into the edge splitter, and the rough edges fall away into a container for reprocessing [7,8].

In this research, HSC™ anode substrates were fabricated using commercially available NiO and 8 mol % yttria-stabilized zirconia (YSZ) powders in a desired ratio (50 vol % Ni + 50 vol % YSZ after the reduction in the anode). The average diameter of NiO particles was  $1.1\ \mu\text{m}$  and that of YSZ was  $0.3\ \mu\text{m}$ . Pore former was added to achieve the desired porosity. Anode barrier layer was applied over the HSC™ anode substrate by wet powder spraying. A suspension of NiO and YSZ powder was prepared by mixing the powders in ethanol with binder for 12 h and sprayed over the substrate using a commercially available air spray gun. The anode active layer was applied over the anode barrier layer. The anode active layer slurry was prepared by mixing NiO and YSZ in alpha-terpineol with binder for 24 h and then it was screen-printed over the anode barrier layer. The electrolyte slurry was prepared by mixing YSZ powders and sintering aids in alpha-terpineol with binder for 4 h, which was applied over the anode active layer by screen-printing. For the preparation of the cathode active layer slurry, Ca-doped  $\text{LaMnO}_3$  (LCM) and YSZ powders were mixed and milled for 12 h in alpha-terpineol with the desired amount of pore former and binder. The average diameter of LCM particles was  $0.9\ \mu\text{m}$ . After mixing, the cathode active layer was screen-printed on top of the electrolyte layer. The slurry for the cathode current collector was prepared by mixing LCM powder for 4 h with the desired amount of pore former and binder in alpha-terpineol. The slurry was then applied on top of the cathode active layer by screen-printing. The cell fabrication was completed by cofiring the green-state cells in air at  $1340^\circ\text{C}$  for 2 h.

**2.2 Cell Testing.** A single cell test setup is comprised of two alumina tubes with the cell sandwiched between them. A gold gasket was placed on the cathode side, and a mica gasket was used on the anode side to seal and prevent direct contact between the cell and the ceramic tube. A glass paste was applied between the two alumina tubes to ensure a tight seal, and the assembled test setup was loaded into the furnace. Silver mesh was used as a current collector on the cathode side and nickel mesh on the anode side. On each side, one wire was used as a current lead and the other as a voltage-measurement lead. Humidified hydrogen was circulated over the anode, and air was circulated over the cathode. The flow rate of fuel was 300 ml/min and that of air was 1 l/min. Hydrogen was bubbled through water, and the water vapor composition in the fuel was varied by controlling the water-bubbler temperature to simulate various fuel utilization conditions under the constant fuel flow rate. All the gas tubing for fuel flow was heated to prevent the condensation of water vapor. Electrochemical measurements were made with the Princeton Applied Research PARSTAT® 2273 potentiostat and impedance analyzer and the KEPCO power amplifier.

**2.3 Microstructure Characterization.** The cells were sectioned and impregnated with epoxy in vacuum. After the epoxy hardened, they were polished down to  $1\ \mu\text{m}$ , and the cross sections were examined with a scanning electron microscope (SEM).

### 3 Results and Discussions

To successfully employ the HSC™ anode in a single step cofiring process, it is important to prevent the chemical reaction between the binder of the HSC™ substrate and the solvent of the screen-printed layers. HSC™ anode is formulated with a water-based binder system, and it is seen that the binder (PVAC or polyvinyl acetate) in the HSC™ anode reacts with the solvent (alpha-terpineol) in the screen-printing slurry used in our single step cofiring process. This reaction damages the green-state anode substrate, and it leads to crack formation after firing. To prevent the chemical reaction between the binder in the HSC™ anode and the screen-printing solvent, an anode barrier layer was applied between the HSC™ anode and the screen-printed layers. Systematic experiments investigating the reactivity of the HSC™ anode with various organic solvents showed that the chemical reaction between ethanol and HSC™ anode is slower than that between the alpha-terpineol and the HSC™ anode. In addition, the boiling point of ethanol ( $78^\circ\text{C}$ ) is lower than that of alpha-terpineol ( $219^\circ\text{C}$ ), and fast evaporation of ethanol is beneficial for avoiding chemical reaction. Since ethanol-based ceramic powder suspensions are widely used in wet powder spraying process to form ceramic films [9–13], the anode barrier layer was deposited on top of the HSC™ anode substrate by wet powder spraying using ethanol-based NiO-YSZ powder suspension and commercially available air spray gun. The process parameters for wet powder spraying such as distance to the substrate, air pressure, velocity of the sprayer motion, and the nozzle size were experimentally optimized to obtain the best quality film. The thickness of the film was controlled by the number of layers, and the thickness measurements of the layers after firing in Fig. 2 shows that the thickness of the film is linearly proportional to the number of deposited layers. The microstructure and porosity of the anode barrier layer was engineered to mimic those of the HSC™ anode support by controlling the initial powder size and solids loading of the suspension.

The anode active layer was applied on top of the anode barrier layer for two reasons: to minimize the surface roughness of the anode barrier layer for subsequent electrolyte screen-printing and to improve the cell performance at high fuel utilization conditions. It was found that the surface of the sprayed layer is rougher than that of the screen-printed layer and that it leads to the sintering cracks of the electrolyte when the YSZ electrolyte is directly screen-printed on top of the rough anode barrier layer as shown in Fig. 3. The reason for the cracks in Fig. 3 is considered to be the stress concentration on the curvature of the interface during sintering, and it requires further study. Screen-printing of the anode active layer using alpha-terpineol-based slurry flattens the surface

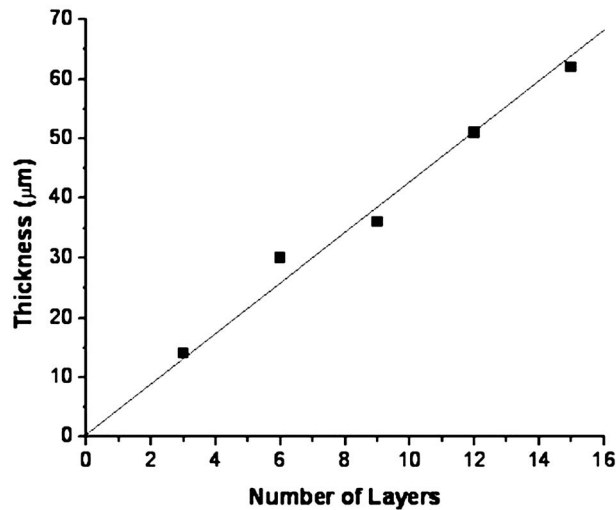


Fig. 2 Thickness of the anode barrier layer versus the number of the sprayed layers

and provides smooth surface for subsequent electrolyte screen-printing to prevent the cracks of the electrolyte due to the surface roughness. In addition, the anode active layer improves the cell performance at high fuel utilization conditions by lowering the anodic activation polarization loss. The anode active layer has a finer and less porous microstructure to increase the number of reaction sites for  $H_2$  oxidation, and our previous work on the effect of the anode active layer on the cell performance showed that the maximum power density at  $800^\circ C$  with the fuel containing 60%  $H_2O$  was improved by 65% by employing a  $20\ \mu m$ -thick anode active layer [14]. This effect will be discussed later.

The cells with different thicknesses of the anode barrier layer were fabricated by a single step cofiring process, and the images of the cofired cells are shown in Fig. 4. It is clearly shown that the crack density decreases with increasing the thickness of the anode barrier layer because the anode barrier layer should have sufficient thickness to prevent the reaction between the HSC™ anode substrate and the screen-printed layers.

Crack-free cell was successfully fabricated with an  $\sim 51\ \mu m$ -thick anode barrier layer, and the microstructure of the cofired cell is shown in Fig. 5. The HSC™ anode support was  $\sim 850\ \mu m$  thick and the measured porosity after reduction was  $\sim 30\%$ . The anode barrier layer was  $\sim 51\ \mu m$  thick and the mea-

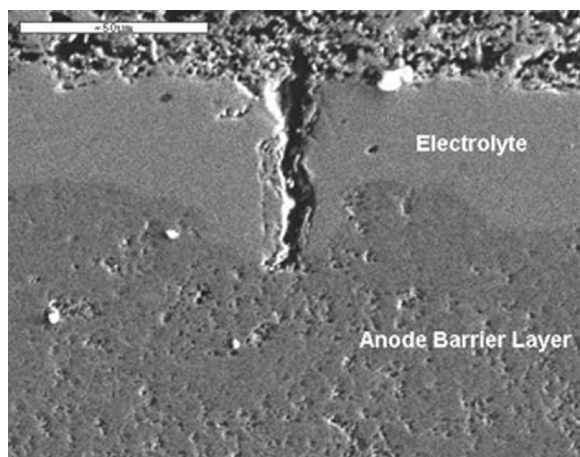


Fig. 3 Cracks of the electrolyte due to the rough surface of the anode barrier layer

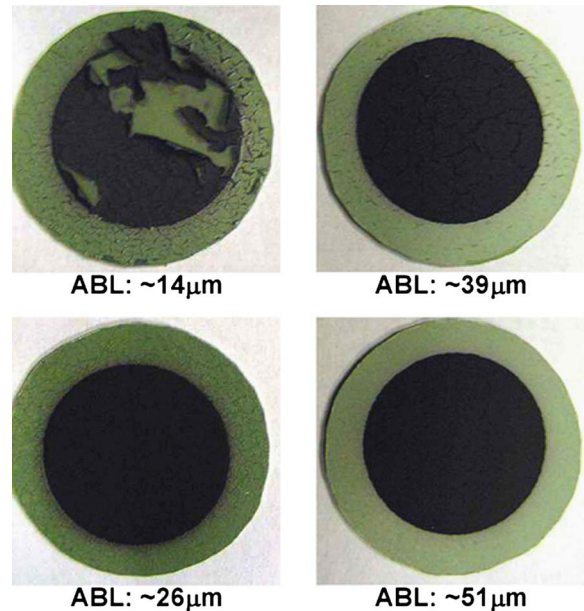


Fig. 4 Cells with different thicknesses of the anode barrier layer

asured porosity after reduction was  $\sim 29\%$ . The anode active layer was  $\sim 20\ \mu m$  thick and its measured porosity after reduction was  $\sim 25\%$ . The electrolyte was  $\sim 15\ \mu m$  thick. The cathode active layer was  $\sim 30\ \mu m$  thick and its measured porosity was  $\sim 31\%$ , and the cathode current collector was  $\sim 50\ \mu m$  thick and its measured porosity was  $\sim 50\%$ .

The cofired cell was electrochemically tested, and Fig. 6 shows the I-V and power density data measured at  $800^\circ C$ ,  $750^\circ C$ , and  $700^\circ C$  with humidified hydrogen (97%  $H_2$ -3%  $H_2O$ ) as fuel and air as oxidant under low fuel utilization condition (fuel flow, 300 ml/min; air flow, 1 l/min). The open circuit voltage (OCV) of the cell was 1.08 V at  $800^\circ C$ , 1.09 V at  $750^\circ C$ , and 1.10 V at  $700^\circ C$ . The OCV was very close to the theoretical value under the test condition, and it indicates that the electrolyte is crack-free and leak-tight. The maximum power densities were  $1.00\ W/cm^2$  at  $800^\circ C$ ,  $0.77\ W/cm^2$  at  $750^\circ C$ , and  $0.53\ W/cm^2$  at  $700^\circ C$ . In our previous work, it was shown that the cathodic activation polarization is one of the dominant polarization losses at low fuel utilization and that it is strongly dependent on the sintering temperature, which determines the microstructure of the cathode ac-

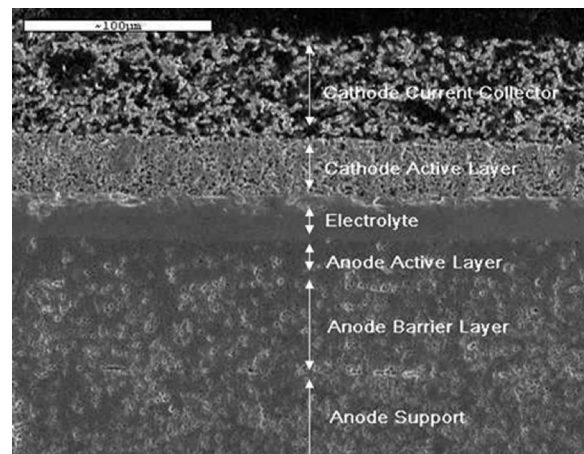


Fig. 5 Microstructure of the cofired cell

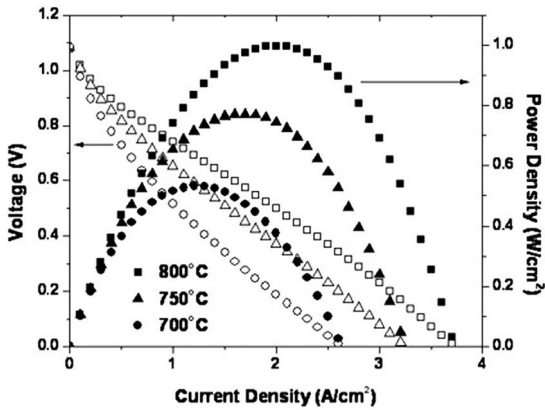


Fig. 6 I-V and power density data measured at 800°C, 750°C, and 700°C with humidified hydrogen (97% H<sub>2</sub>-3% H<sub>2</sub>O) as fuel and air as oxidant

tive layer [1]. Therefore, the performance of the cofired cell at low fuel utilization can be further improved by lowering the sintering temperature and increasing the three phase boundary length of the cathode active layer.

This cell was also tested as a function of fuel utilization at 800°C by simulating various fuel utilization conditions by changing the H<sub>2</sub>O content in the fuel under constant fuel flow rate (300 ml/min). In an operating SOFC stack, the fuel composition changes along the flow channel over the anode surface because the fuel (H<sub>2</sub>) is electrochemically oxidized along the anode channel, and the anode fuel stream is diluted by the reaction product (H<sub>2</sub>O). Fuel utilization is defined as the fraction of the input fuel, which is electrochemically utilized, and the additional cell potential loss occurs at high fuel utilization condition near the exit of the flow channel. Therefore, it is important to minimize the cell potential losses at high fuel utilization to achieve high cell performance in a stack. In this experiment, the cell was tested with various compositions of humidified hydrogen fuel to simulate the various fuel utilization conditions occurring in the operating SOFC stacks, and the results are shown in Fig. 7. The maximum power densities of the cell were 0.89 W/cm<sup>2</sup> with 70% H<sub>2</sub>-30% H<sub>2</sub>O, 0.83 W/cm<sup>2</sup> with 50% H<sub>2</sub>-50% H<sub>2</sub>O, and 0.72 W/cm<sup>2</sup> with 40% H<sub>2</sub>-60% H<sub>2</sub>O.

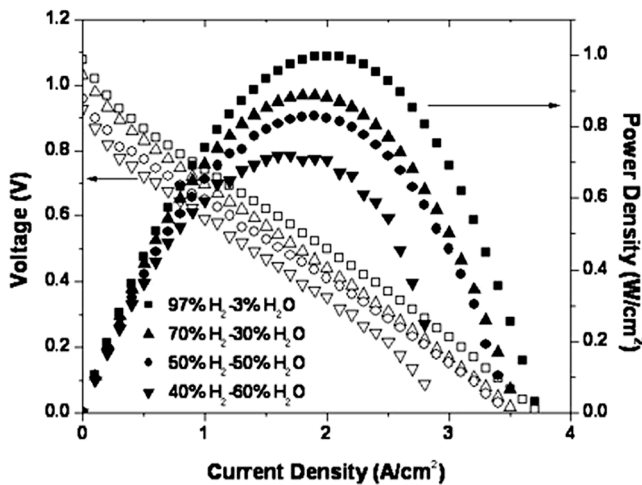


Fig. 7 I-V and power density data measured with various compositions of humidified hydrogen (3-60% H<sub>2</sub>O) as fuel and air as oxidant at 800°C

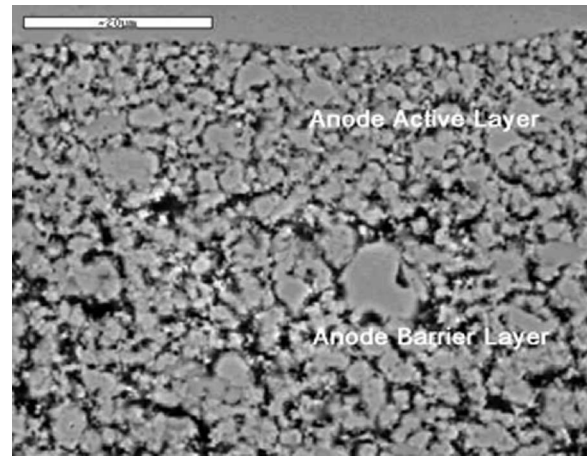


Fig. 8 SEM image of the anode active layer and anode barrier layer

Our previous work showed that without the anode active layer, the performance of the cell drops by 55% when the H<sub>2</sub>O content in the fuel increases from 3% to 60% [15,16]. In this work, the performance drop under the same condition was reduced to 27% by employing the anode active layer. In our previous work on anode reaction kinetics of the single step cofired SOFCs, the analytical model describing the H<sub>2</sub>-H<sub>2</sub>O reaction predicted that the formation of water molecules from adsorbed hydrogen and hydroxyl radical is the rate limiting step in the anodic reaction, and the cell performance at high fuel utilization can be improved by increasing the number of reaction sites [15]. The number of reaction sites is attributed to the triple phase (gas-electrode-electrolyte) boundary (TPB) length in porous, two-phase mixed conducting electrodes; in the anode, the boundary between nickel and zirconia particles works as the TPB. The anode active layer in Fig. 8 has the same composition as the anode substrate but was engineered to have a finer and less porous microstructure than the anode substrate and the anode barrier layer to maximize the TPB length. It was theoretically shown by Tanner et al. [17] that the effective charge-transfer resistance scales as the square root of the grain size of the electrode material. The measured average grain size of the anode active layer was ~1.5 μm, and the measured average pore diameter of the anode active layer was ~0.8 μm, while the measured average grain size of the anode substrate and the anode barrier layer was ~4.0 μm, and the measured average pore diameter of the anode support and the anode barrier layer was ~2.5 μm. As a result, high performance of the cell at high fuel utilization conditions was achieved by employing the anode active layer, which increases the number of reaction sites and lowers the anodic activation polarization loss.

#### 4 Conclusions

In this work, anode-supported planar solid oxide fuel cell based on YSZ electrolyte was successfully fabricated by a single step cofiring process using HSC<sup>TM</sup> anode substrate. The chemical reaction between the HSC<sup>TM</sup> anode substrate and screen-printed layers was prevented by applying the anode barrier layer by means of a wet powder spraying process. The anode active layer with finer and less porous microstructure was screen-printed over the anode barrier layer to flatten the surface of the anode barrier layer for subsequent electrolyte screen-printing and to increase the TPB length for improved cell performance at high fuel utilization. The microstructure and the OCV of the cell showed that the cell was crack-free and leak-tight. The cell showed stable performance in the electrochemical test between 700°C and 800°C with humidified hydrogen (97% H<sub>2</sub>-3% H<sub>2</sub>O) as fuel and air as oxidant. High performance of the cell was achieved at high fuel utilization

since the anode active layer increased the number of reaction sites and lowered the anodic activation polarization loss. The material system and fabrication processes presented in this work offers great advantage in low-cost and high-volume SOFC production, and it can be the basis for successful commercialization of the SOFC technology.

### Acknowledgment

The financial support from BTU International is gratefully acknowledged.

### References

- [1] Yoon, K. J., Zink, P., Gopalan, S., and Pal, U. B., 2007, "Polarization Measurements on Single-Step Co-Fired Solid Oxide Fuel Cells (SOFCs)," *J. Power Sources*, **172**(1), pp. 39–49.
- [2] Yoon, K. J., Gopalan, S., and Pal, U. B., 2007, "High Performance Single Step Co-Fired Solid Oxide Fuel Cells," *Mater. Res. Soc. Symp. Proc.*, **972**, pp. 149–154.
- [3] Yoon, K. J., Huang, W., Ye, G., Gopalan, S., Pal, U. B., and Seccombe, D. A., Jr., 2007, "Electrochemical Performance of Solid Oxide Fuel Cells Manufactured by Single Step Co-Firing Process," *J. Electrochem. Soc.*, **154**(4), pp. B389–B395.
- [4] Yoon, K. J., Zink, P., Pal, U. B., Gopalan, S., and Seccombe, D. A., Jr., 2007, "High Performance Low Cost Co-Fired Solid Oxide Fuel Cells," *ECS Trans.*, **7**(1), pp. 579–588.
- [5] Buchkremer, H. P., Diekmann, U., De Haart, L. G. J., Kabs, W., Stimming, U., and Stover, D., 1997, "Advances in the Anode Supported Planar SOFC Technology," *Proceedings of the Fifth International Symposium on Solid Oxide Fuel Cells (SOFC-V)*, Aachen, Germany, pp. 160–170.
- [6] Patcharavorachot, Y., Arpornwichanop, A., and Chuachuensuk, A., 2008, "Electrochemical Study of a Planar Solid Oxide Fuel Cell: Role of Support Structures," *J. Power Sources*, **177**(2), pp. 254–261.
- [7] Ragan, R. C., 1996, "Process for Producing Low Shrink Ceramic Composition," U.S. Patent No. 5,518,969.
- [8] Belko, W. C., and Ragan, R. C., 1998, "Process for Producing Low Shrink Ceramic Bodies," U.S. Patent No. 5,769,917.
- [9] Schuller, E., Vaben, R., and Stover, D., 2002, "Thin Electrolyte Layers for SOFC Via Wet Powder Spraying (WPS)," *Adv. Eng. Mater.*, **4**(9), pp. 659–662.
- [10] Oishi, N., Yoo, Y., and Davidson, I., 2007, "Fabrication of Gas Electrodes by Wet Powder Spraying of Binder-Free Particle Suspensions Using a Pulse Injection Process," *J. Am. Ceram. Soc.*, **90**(5), pp. 1365–1369.
- [11] Sammes, N. M., Brown, M. S., and Ratnaraj, R., 1994, "Wet Powder Spraying of a Cermet Anode for a Planar Solid Oxide Fuel Cell System," *J. Mater. Sci. Lett.*, **13**(15), pp. 1124–1126.
- [12] Ruder, A., Buchkremer, H. P., Jansen, H., Mallener, W., and Stover, D., 1992, "Wet Powder Spraying—A Process for the Production of Coatings," *Surf. Coat. Technol.*, **53**(1), pp. 71–74.
- [13] Jansen, H., Buchkremer, H. P., Stover, D., and Wippermann, K., 1993, "Cell Component Fabrication by Wet Powder Spraying [SOFC]," *Proceedings of the Third International Symposium on Solid Oxide Fuel Cells*, Honolulu, HI, pp. 752–755.
- [14] Yoon, K. J., Gopalan, S., and Pal, U. B., 2008, "Effect of Anode Active Layer on Performance of Single Step Co-Fired Solid Oxide Fuel Cells," *J. Electrochem. Soc.*, **155**(6), pp. B610–B617.
- [15] Yoon, K. J., Gopalan, S., and Pal, U. B., 2007, "Effect of Fuel Composition on Performance of Single-Step Cofired SOFCs," *J. Electrochem. Soc.*, **154**(10), pp. B1080–B1087.
- [16] Yoon, K. J., Gopalan, S., and Pal, U. B., 2007, "Anode Polarization Effects in Single Step Co-Fired Solid Oxide Fuel Cells," *ECS Trans.*, **7**(1), pp. 565–572.
- [17] Tanner, C. W., Fung, K.-Z., and Virkar, A. V., 1997, "The Effect of Porous Composite Electrode Structure on Solid Oxide Fuel Cell Performance," *J. Electrochem. Soc.*, **144**(1), pp. 21–30.